Chloroplast/thylakoid-rich material

Sutcharit, Pomarat; Wattanakul, Jutarat; Price, Ruth; di Bari, Vincenzo; Gould, Joanne; Yakubov, Gleb; Wolf, Bettina; Gray, David A.

DOI:
10.1016/j.foodres.2023.112472

Chloroplast/Thylakoid-rich Material: A Possible Alternative to the Chemically Synthesised Flow Enhancer Polyglycerol Polyricinoleate in Oil-Based Systems

Poramat SUTCHARIT[a] (poramat.sucharit@nottingham.ac.uk), Jutarat WATTANAKUL[a, b] (jutarat.wattanakul@nottingham.ac.uk), Ruth PRICE[a] (ruth.price@nottingham.ac.uk), Vincenzo Di Bari[a] (vincenzo.dibari@nottingham.ac.uk), Joanne GOULD[a] (joanne.gould@nottingham.ac.uk), Gleb YAKUBOV[a] (gleb.yakubov@nottingham.ac.uk), Bettina WOLF[c] (B.wolf@bham.ac.uk), David A. GRAY[a*] (David.gray@nottingham.ac.uk)

[a] Division of Food, Nutrition and Dietetics, School of Biosciences, University of Nottingham, Sutton Bonington Campus, Loughborough LE12 5RD, United Kingdom.

[b] Department of Food Sciences and Technology, Faculty of Home Economics Technology, Rajamangala University of Technology Krungthep, Bangkok, 10120, Thailand.

[c] School of Chemical Engineering, University of Birmingham, Edgbaston Campus, Birmingham B15 2TT, United Kingdom.

*Corresponding author's telephone: +44 (0) 115 951 6147

Abstract

Chloroplasts are abundant organelles in a diverse range of plant materials; they are predominantly composed of multicomponent thylakoid membranes which are lipid and protein rich. Intact or unravelled thylakoid membranes should, in principle, have interfacial activity, but little has been published on their activity in oil-in-water systems, and nothing on their performance on an oil continuous system. In this work different physical methods were used to produce a range of chloroplast/thylakoid suspensions with varying degrees of membrane integrity. Transmission electron microscopy revealed that pressure homogenisation led to the greatest extent of membrane and organelle disruption compared to less energy intensive preparation methods The ability of the derived materials to modulate the flow behaviour of a chocolate model system (65% (w/w) sugar/ sunflower oil (natural amphiphiles removed) suspension) was investigated by acquiring rheological parameters. All chloroplast/thylakoid preparations reduced yield stress, apparent viscosity, tangent flow point and cross over point in a concentration-dependent fashion, although not as significantly as polyglycerol polyricinoleate applied at a commercially relevant concentration in the same chocolate model system. Confocal laser scanning microscopy confirmed presence of the alternative flow enhancer material at the sugar surfaces. This research reveals that low-energy processing methods that do not extensively disrupt thylakoid membranes are applicable to generating materials with marked capacity to affect the flow behaviour of a chocolate model system. In conclusion, chloroplast/thylakoid materials hold strong potential as natural alternatives to synthetic rheology modifiers for lipid-based systems such as PGPR.

Key words: Chocolate; Rheology; Casson model; Emulsifier; Yield stress; Apparent Viscosity; chloroplast; thylakoid membranes

Abbreviations

η_{40}: Apparent Viscosity at 40 seconds^{-1} (Pa s)

BCRF: Burst Chloroplast-rich Fraction (wet sample)

B-CRF: Burst Chloroplast-rich Fraction (dried powder sample)

COP: Cross Over Point (Pa)

η_c: Casson Viscosity (Pa s)

σ_c: Casson Yield Stress (Pa)

CP: Combined Pellet, P1 and P2 (wet sample)

DP: Diluted Pellet (wet sample)

DP-CRF: Diluted Pellet Chloroplast-rich Fraction (dried powder sample)

J-Method: Juicing Method

P1: Pellet 1 (First Centrifugation) (wet sample)

P2: Pellet 2 (Second Centrifugation) (wet sample)

P-CRF: Pellet Chloroplast-rich Fraction (dried powder sample)

PGPR: Polyglycerol Polyricinoleate

S-CRF: Rhodamine B Stained Chloroplast-rich Fraction (dried powder sample)

$\dot{\gamma}$: Shear Rate (s^{-1})

66 σ: Shear Stress (Pa)

67 SJ: Spinach Juice

68 s/o: Sugar-in-Oil Suspension

69 SN1: Supernatant 1 (First Centrifugation)

70 SN2: Supernatant 2 (Second Centrifugation)

71 TFP: Tangent Flow Point (Pa)

72 WBSJ: Water Blended Spinach Juice (wet sample)

73 WBTRF: Water Blended Thylakoid-rich Fraction (wet sample)

74 WB-Method: Water Blending Method

75 τ_5: Yield Stress at 5 seconds^{-1} (Pa)

76

1. Introduction

Chocolate is one of the most popular and highly consumed confections products worldwide. Originating from Central and South America, roasted and ground cacao beans (*Theobroma cacao* L.) have been used in various confectionery products such as chocolate bars and drinks. Chocolate consists mainly of ground, roasted cocoa nibs, cocoa butter and milled sugar (Beckett, 2009). The flow behaviour of molten chocolate is highly dependent on manufacturing steps, such as mixing, refining, conching, tempering and moulding (Shafi, Reshi, Aiman, & Bashir, 2018), and formulation such as solids particle size and lipid fraction (Afoakwa, Paterson, & Fowler, 2007; Beckett, 2009). Frequently formulations also contain emulsifiers to tune the rheological properties of molten chocolate for moulding or enrobing processes (Afoakwa, 2016). Parameters such yield stress (σ), apparent viscosity (η_a), tangent flow point (TFP) and cross over point (COP) are commonly used in practice to quantify the flow behaviour of chocolate (Afoakwa, Paterson, Fowler, & Vieira, 2009; Beckett, 2009; De Graef, Depypere, Minnaert, & Dewettinck, 2011; Peker, Suna, Tamer, & Copur, 2013; Servais, Ranc, & Roberts, 2003).

In chocolate the hydrophilic part of an emulsifier molecule associates with the sugar particle surfaces while the hydrophobic part extends into the continuous cocoa butter phase. One of the most common emulsifiers used in confectionery products to control yield stress (σ) is polyglycerol polyricinoleate (PGPR, Food label - E476) (Schantz & Rohm, 2005; Sözeri Atik, Bölük, Toker, Palabiyik, & Konar, 2020). PGPR is a chemical compound obtained through acid esterification of castor oil in the presence of polyglycerol (Wilson, Van Schie, & Howes, 1998). Although PGPR has been deemed as safe by the Joint FAO/WHO Expert Committee on Food Additives (FECFA), the Scientific Committee of Food (SCF) (Ministers, 2002) and 'generally recognised as safe' (GRAS) by the Food and Drugs Administration (FDA) as well as deemed safe following a recent re-evaluation by the European Food Safety Authority (EFSA Panel on Food Additives Nutrient Sources added to Food et al., 2017), restrictions on quantities used in confectionery products are still being carefully monitored: 0.3% (w/w) in the US; 0.5% (w/w) in Canada, Australia, New Zealand and the European Union (EU) (Quest International, 1997).

Nevertheless, consumers increasingly prefer clean-label products (Osborn, 2015) which drives the confectionery industry to look for a natural alternative to the synthetic PGPR, i.e., a natural amphiphile that is effective in controlling the yield stress of chocolate.

Chloroplasts, organelles ubiquitous in the biosphere that convert sunlight energy into chemical energy (in the form of sugar), are an abundant source of interfacial-active galactolipids. With a diameter between 3 – 10 µm, chloroplasts contain three different membrane systems: the outer- and inner-envelope membranes, and the thylakoid membrane (Block, Dorne, Joyard, & Douce, 1983). Enriched with macro- and micro-nutrients (Mohamed A. Gedi et al., 2017; M. A. Gedi et al., 2019; Syamila, Gedi, Briars, Ayed, & Gray, 2019; Torcello-Gomez et al., 2019; Jutarat Wattanakul et al., 2019), chloroplasts were reported to possess interfacial-active properties which have been shown to retard fat digestion, (Albertsson et al., 2007; Ostbring et al., 2018) and stabilise oil-in-water emulsions (Rayner, Emek, Gustafssona, Albertsson, & Albertsson, 2011; Rayner, Ljusberg, et al., 2011; Tenorio, de Jong, Nikiforidis, Boom, & van der Goot, 2017). In a separate study, the extracted chloroplast lipids enhanced the flow properties in a moderately concentrated sugar-in-oil-suspension (Mohamad, Gray, & Wolf, 2020). The objective of this work was to assess the ability of intact chloroplast membranes, a lesser refined natural system than extracted lipids avoiding the use of organic solvents (e.g., hexane, chloroform and/or methanol) during preparation, to replace PGPR in future chocolate formulations. In contrast to Mohamad et al. (2020), a highly concentrated sugar-in-oil (s/o) suspension (65% (w/w) sugar, equivalent to 53% (v/v)), was recently developed for the comparative assessment of commercial PGPR samples by Price, Gray, Watson, Vieira, and Wolf (2022); this model was used as the chocolate model system. The naturally present amphiphiles in the oil phase were removed prior to preparing the suspension to ensure the rheological parameter values could be related to the action of the chloroplast/thylakoid systems alone. Such systems were prepared from spinach leaf, an easy-accessible green leaf tissue system applied in previous related work (Mohamed A. Gedi et al., 2017; Mohamad et al., 2020; Jutarat Wattanakul et al., 2022) using juicing and blending methods. It was

hypothesised that the loss of chloroplast integrity would be accompanied by an increase in de-stacked, liberated thylakoid membranes which in turn would increase the interfacial activity of the material per unit mass and ultimately reduce the yield stress in the s/o suspension. Based on microscopy and particle size analysis a subset of chloroplast/thylakoid systems of varying degrees of integrity was selected and applied in the suspensions. Their rheological properties were then compared to those of suspension containing PGPR as interfacial-active additive and the results interpreted in conjunction with micrographs acquired on the suspensions.

2. Materials and Methods

2.1 Materials

A total of 9 kg of spinach leaves (*Spinacia oleracea* L.) was purchased from a local store (Tesco, Nottingham, United Kingdom) and immediately stored at 4°C (Polysec Coldrooms Ltd, Worcester, United Kingdom) until use. Sunflower oil (*Helianthus annus* L.) was also purchased from a local store (Sainsburys, Nottingham, United Kingdom) and stored at room temperature in the dark. Polyglycerol polyricinoleate (PGPR), Palsgaard 4150 and Grindsted 90, was gifted by Palsgaard A/S (Juelsminde, Denmark) and Danisco A/S (Copenhagen, Denmark), respectively. EM grade glutaraldehyde, cocadylate buffer, osmium tetroxide, uranyl acetate, ethanol, propylene oxide, resin solutions, sodium hydroxide and lead citrate were kindly provided by the Nanoscale and Microscale Research Centre at the University of Nottingham (Nottingham, United Kingdom). Magnesium silicate (Florisil®), rhodamine B, isopropanol and n-heptane were of HPLC grade and purchased directly from Sigma-Aldrich (Darmstadt, Germany) and Thermo Fisher Scientific (Waltham, Massachusetts, United States).

2.2 Methods

2.2.1 Preparation of Chloroplast Fractions via Juicing Method

A juicing method was applied to prepare a chloroplast-rich pellet from spinach leaves, see also Fig. 1. The spinach leaves were weighed, washed thoroughly with tap water, and divided into batches of approximately 1 kg. Before proceeding to the juicing process, the leaves were partially dried using a domestic 'salad spinner'. Leaves were juiced using a vegetable juicer (Angel Juicer 7500 Angel Juicer Co., Ltd, Busan, South Korea), filtered (75 μm) and centrifuged (Beckman J2-21, Beckman Coulter, London, United Kingdom) (17,700 g, 10 minutes, 4°C) to obtain a chloroplast-rich pellet (Torcello-Gomez et al., 2019). Spinach juice (SJ) was used as the control for chloroplast native state while the centrifugation step was repeated twice to obtain supernatant samples (SN1, SN2), and pellet samples (P1, P2).

One lot of pellet samples P1 and P2 was combined, referred to as CP or combined pellet sample, and further processed as follows. CP (40 g) was transferred to a conical flask with 1 litre of ultra-pure water (1:25 ratio) and thoroughly mixed with a magnetic stirrer (RCT digital, IKA-Werke, Staufen, Germany) in the dark (600 rpm, 2 hours, 4°C). The diluted pellet (DP) was then homogenised at 100 MPa (1,000 bar, 1 passage) using a high-pressure homogeniser (GEA Niro Soavi high-pressure homogeniser, NS1001L2K, GEA, Düsseldorf, Germany). The pre-homogenised diluted pellet (DP) and post-homogenised juice, termed burst chloroplast-rich fraction (BCRF), were collected, packed in a vacuum sealed bags and stored at -20°C until use.

2.2.2 Preparation of Thylakoid Fraction via Water Blending

As an alternative to the juicing method, a water blending method adapted from literature (Ostbring et al., 2018; Rayner, Emek, et al., 2011; Rayner, Ljusberg, et al., 2011) was applied, see also Fig. 2. To 100 g of spinach leaves, 200 g of ultra-pure water (18.2 MΩcm Milli-Q Direct water, Merck, Darmstadt, Germany) was added (1:2 ratio), homogenised at full power using a blender (Kenwood BLX510, United Kingdom) for 5 minutes, filtered (75 μm) to obtain water blended spinach juice (WBSJ)

and centrifuged (6,400 g, 10 minutes, 4°C). The pellet was collected, diluted at 1:2 ratio with ultra-pure water, thoroughly vortex and centrifuged (17,700 g, 15 minutes, 4°C) to obtain water blended thylakoid-rich fraction (WBTRF) as the pellet at the bottom of the centrifuge tube. The filtered water blended spinach juice (WBSJ) and pellet (WBTRF) were collected, packed in vacuum sealed bag and store at -20°C until use.

2.2.3 Lipid Extraction

The process of total lipid extraction was performed following the protocol outlined by Folch et al. (1957) and Bligh and Dyer (1959) with minor adjustments. To 0.1 g of the freeze-dried sample, 1.2 ml of 2:1 chloroform to methanol solution (CHCl3: MeOH) was added and vortex (1 min). Prior to centrifugation (3,000 rpm, 10 mins, 4°C), 0.9% sodium chloride (0.6 ml) was added and vortex for 1 minute. The lower phase (lipid extract) was collected along with an addition of 1.2 ml 2:1 CHCl3: MeOH, vortex (1 min) and centrifuged (3,000 rpm, 10 mins, 4°C). The extraction process was repeated for three times. The accumulated lipid extracts then get centrifuged (3,000 rpm, 10 mins, 4°C), extracted, filtered (0.45 µm, 13 mm) into a tared glass bijoux bottle and dried using nitrogen gas.

2.2.4 Total Chlorophyll Analysis

Dried lipid extracts were dissolved with acetone (1 ml), vortex (1 min) and perform further 2-step serial dilution with acetone (1:250, 1:1,000, 1:2,000, 1:10,000) until the absorbance values fall within the range of 0.1 – 1.0A. The total chlorophyll a (*Chl a*) and b (*Chl b*) pigment was measured using UV-Vis Spectrophotometer (Genesys 10S, Thermo Fisher Scientific, Waltham, Massachusetts, 57 United States) at 662 and 645 nm respectively (Gedi et al., 2017, Torcello-Gomez et al., 2019). The concentration of *Chl a* and *b* was calculated using equations (Eq. 3.1 and Eq. 3.2) suggested earlier by

Lichtenthaler (2001). The total chlorophyll content is calculated as the sum of both *Chl a* and *b* (Eq. 3.3).

$$Chl\ a\ (\mu g/g) = (11.24 \times A_{661.6}) - (2.04 \times A_{644.8}) \quad \text{(Eq. 3.1)}$$

$$Chl\ b\ (\mu g/g) = (20.31 \times A_{644.8}) - (4.19 \times A_{661.6}) \quad \text{(Eq. 3.2)}$$

$$Total\ Chlorophyll\ Content = Chl\ a + Chl\ b \quad \text{(Eq. 3.3)}$$

2.2.5 Galactolipids Analysis

The analysis of galactolipids (monogalactosyldiacylglycerol (MGDG) and digalactosyldiacylglycerol (DGDG)) was performed using the high-performance thin layer chromatography (HPTLC) technique.

To the dried lipid extracts, 1 ml of 2:1 chloroform to methanol solution (CHCl3: MeOH) was added. Both samples and standards were transferred to the same silica gel thin layer chromatography (TLC) plate (Merck, Darmstadt, Germany) using the Hamilton syringe (Merck, Darmstadt, Germany) and Linomat 5 (Camag, Muttenz, Switzerland). The injection setting was set to 1 µl (5 bars) and repeated to reach the desired concentration. The plates were developed in a twin-trough chamber (Camag, Muttenz, Switzerland) using the mobile phase (47.5: 10: 1.25, chloroform: methanol: water, v/v/v) for 10 mins prior to drying in the fume hood (10 mins). Plate derivatization was performed using Chromatogram Immersion Device 3 (Camag, Muttenz, Switzerland). In this experiment, thymol solution is use to selectively stain the galactolipids (MGDG & DGDG) avoiding the interference that may occur during the densitometric analysis by the HPTLC.

The thymol solution is prepared as follow. To 1 g of thymol, 190 ml of ethanol was added following with a slow addition of 10 ml of sulphuric acid (96%) – the ice water bath was used to control and avoid rapid exothermic reactions. After the derivatization, the plate was left to dry in the fume

hood (10 mins) and oven heated for 10 minutes at 110°C before the densitometric analysis. The quantitative analysis of HPTLC (densitometric analysis) was perform using TLC Visualiser 2 (Camag, Muttenz, Switzerland) and VisionCATs software (Camag, Muttenz, Switzerland). Image acquisition of TLC plates were obtained under white light, 64 254 and 366 nm respectively. The determination of galactolipids was calculated using the standard curve plotted from the MGDG and DGDG standards.

2.2.6 Particle Size Analysis

A Horiba Partica LA-960 Laser Scattering Particle Size Distribution Analyzer (Kyoto, Japan) equipped with a tempax glass flow cell (Kyoto, Japan) was used to analyse the particle size distribution of the chloroplast/thylakoid preparations. Every measurement was performed with two light sources (405 and 650 nm) and the scattering patterns analysed following the Mie theory, utilising the equipment's software. Triplicate measurements were carried out with agitation, circulation and the transmission settings at level 2, 5 and between 70 – 95%, respectively. Relevant statistical analyses were carried out as detailed later on.

2.2.7 Microstructure Analyses of Prepared Chloroplast/Thylakoid Preparations

2.2.7.1 Light Microscopy

Light micrographs were acquired with a transmitted light microscope (Nikon Eclipse Ci, Shinagawa, Tokyo, Japan) to validate the light scattering particle size data and understand whether the chloroplasts were intact or broken. All light micrographs were taken using phase contrast and a 40X objective lens. Based on 3 images and a total of 15 chloroplast structures per sample, chloroplast particle size was estimated utilising image analysis software Fiji (Schindelin et al., 2012).

2.2.7.2 Transmission Electron Microscopy

Fresh chloroplast/thylakoid preparations were fixed with 3% EM grade glutaraldehyde in 0.1M cacodylate buffer and stored overnight at 4°C. Washing steps (2 changes, 0.1M cacodylate buffer, 5 minutes) were performed and the preparations stored in 0.1M cacodylate buffer (1 ml, 4°C, dark) before post-tissue-fixation with 1% osmium tetroxide in 0.1M cacodylate buffer (2 hours, room temperature). Samples were then washed (2 changes, distilled water, 10 minutes), stained en bloc (1% aqueous uranyl acetate, overnight, 4°C, dark), washed (3 changes, distilled water, 5 minutes) and dehydrated with 50%, 70%, 90% (2 x 10 minute for each) and 100% ethanol (3 x 15 minutes), respectively. To further remove water from the samples, propylene oxide (100%) was added (3 changes, 15 minutes, room temperature) followed by the addition of propylene oxide : resin (24 g TLV Resin, 26 g TLV Hardener VH2) solution at 3:1 ratio (1 hour, room temperature) and 1:1 ratio (overnight with lids off, room temperature), respectively. A pure resin preparation (TAAB Low Viscosity Resin – hard recipe) was then added (2 changes, 1 hour) before embedding in the oven at 70°C for 48 hours. Samples were then sectioned with a diamond knife at 90 nm thick using a Leica EM UC6 (Leica Biosystems, Wetzlar, Germany), placed on a 200-mesh carbon support copper grid and stained with lead citrate. Grids were analysed using a Tecnai Bio-TWIN T12 Biotwin transmission electron microscope (TEM) (FEI Company, Eindhoven, The Netherlands) at an accelerated voltage of 100 kV. Images were captured using a MegaView SIS camera at X9900 magnification.

2.2.8 Sugar-in-oil Suspensions Preparation and Analyses

2.2.8.1 Preparation of Sugar-in-Oil Suspensions

The first step of preparing the sugar-in-oil (s/o) suspensions involved the removal of naturally present interfacial-active components in the continuous oil phase material, i.e., sunflower oil. The sunflower oil was chosen for this experiment to create a simplified chocolate model making it easier

to interpret the effect of added complex chloroplast material. Moreover, various studies have also used the sunflower oil as a continuous phase in s/o suspension to test the impact of different emulsifiers (Manasi et al., 2019; Price et al., 2022). The oil was treated with 4% (w/w) magnesium silicate (Florisil®) at 600 rpm for 30 minutes followed by centrifugation (2,700 g, 30 minutes, 20°C) to remove the Florisil®. The treated oil, referred to simply as oil or sunflower oil in the following, was stored in an amber glass bottle at 5°C in the dark until use. The icing sugar was also pre-treated by drying in a vacuum oven at 60°C for 24 hours and stored in an air-tight container until use. The particle size distribution of the dried icing sugar is provided in Appendix Fig. A.1 ($d_{4,3}$: 35.6 ± 2.3 µm).

The chloroplast samples chosen for incorporation into the s/o suspension included CP, DP and BCRF. These materials were prepared as described earlier followed by freezing at -80°C for 24 h (Denley, Massachusetts, United States), freeze-drying (Edwards, Burgess Hill, England) for 7 days, grinding using a granite pestle and mortar, sieving (106 µm), vacuum-packaging and storage at -20°C until use. Freeze-dried CP, DP and BCRF material is in the following referred to as P-CRF (pellet chloroplast-rich fraction), DP-CRF (diluted pellet chloroplast-rich fraction) and B-CRF (burst chloroplast-rich fraction).

The s/o suspensions were then prepared as follows. 75 g of purified sunflower oil was added to a beaker containing dried chloroplast material (P-CRF, DP-CRF or B-CRF) (at the appropriate level for the final suspension to contain 0.5, 1.0 or 2.0% w/w of this material) and stirred at 600 rpm for 1 h in the dark. The stirrer was removed, 75 g of dried icing sugar mixed in using a spatula followed by using a high shear mixer (Silverson mixer L5 series) (8,000 rpm, 4 minutes, on ice). To simulate the amount of particles in chocolate (65 – 75% w/w) (Afoakwa et al., 2007), the samples were centrifuged (2,700 g, 10 minutes, 20°C), and the appropriate amount of oil supernatant removed to obtain a 65% (w/w) (equivalent to 53%, v/v) sugar-in-oil suspension. PGPR stabilised suspensions were prepared following the same protocol, replacing the chloroplast material with PGPR 4150 and G90 (0.1, 0.2 or 0.4% w/w in the final suspension).

294

295 **2.2.8.2 Rheological measurements**

296 Rheological measurements were performed using a stress-controlled rheometer (Physica
297 MCR 301, Anton Paar, Graz, Austria) equipped with a serrated cup and bob geometry (CC27, Anton
298 Paar, Graz, Austria). All measurements were performed in triplicate for each sample at a constant
299 temperature of 20°C. Unidirectional measurements were set up to follow a ramp-down protocol
300 (1,000 Pa to 0.01 Pa) (Price et al., 2022) and oscillatory measurements to follow a ramp-up protocol
301 (0.01 Pa to 100 Pa) at the constant angular frequency (ω) of 10 rad/s. For both types of measurements
302 10 logarithmically spaced data points were recorded per decade of stress, with each stress value
303 applied for 10 s prior to data capture.

304 The data from the unidirectional stress controlled (τ versus $\dot{\gamma}$) measurements was analysed
305 using RheoCompass software (Anton Paar, Frazm, Austria). The Casson model (Eq. 1) was used to
306 describe the flow behaviour of the model chocolate system.

307 $$\sigma^{0.5} = \sigma_c^{0.5} + (\eta_c \dot{\gamma})^{0.5} \quad \text{(Eq. 1)}$$

308 σ and $\dot{\gamma}$ is shear stress and shear rate, σ_c and η_c indicates the Casson yield point and Casson
309 viscosity, respectively (Rao, 2014). In addition, the data were used to determine apparent viscosity at
310 40 s^{-1} (η_{40}) and shear stress at 5 s^{-1} (τ_5) taken to represent the yield stress (σ) (Servais et al., 2003).
311 For sake of clarity, τ_5 will be referred to as the "shear stress value at 5 s^{-1} (τ_5)". In additional, the cross
312 over point (COP) and tangent flow point (TFP) were determined from the oscillatory measurements,
313 more specifically the dependency of the storage (G') and loss moduli (G'') on oscillatory stress. The
314 determination of both COP and TFP was found to be system specific and is described in detail when
315 introducing the results.

316

2.2.8.3 Confocal Microscopy

Filtered (75 μm) spinach juice (Section 2.2.1) was stained with rhodamine B (0.01 g/L) and stirred at 600 rpm, 1 hour at room temperature. The objective of this staining is to stain the protein components on the chloroplast and thylakoid structures (integral and peripheral membrane proteins) prior to centrifugation. The sample was then centrifuged (17,700 g, 10 minutes, 4°C), frozen (24 hours, -80°C) (Denley, Massachusetts, United States), freeze-dried (7 days) (Edwards, Burgess Hill, England), ground and sieved (106 μm) to obtain stained chloroplast-rich fraction (S-CRF). The stained powder was then vacuum-packed and stored at -20°C until a suspension sample was prepared containing this powder. The suspension was prepared as described in 2.2.7.1 containing 1.0% S-CRF and the reduced sugar level of 50% to facilitate imaging. A small sample of the suspension was dropped onto a slide and gentle spread out to maximise the clarity of microstructure. A Zeiss LSM 880 laser confocal scanning microscope (Carl Zeiss AG, Oberkochen, Germany) installed with a red channel laser (561 nm) was used to image the microstructure. With the peak region selected for each slide, multiple images were taken with a X63 objective lens and z-planes thicknesses of 0.5 and 0.2 μm.

2.2.9 Statistical Analysis

All measurements were conducted in triplicate measurements and the sample mean ($\bar{x}$), standard deviation (SD) and standard error (SE) calculated. Using IBM SPSS Statistic 25, the Student t-test was performed at $p \leq 0.05$ significant level or 95% confidence limit for every data set.

3. Results and Discussion

3.1. Microstructure of Chloroplast/thylakoid materials

339 An overview of the microstructures found in the various chloroplast/thylakoid materials,
340 prepared as summarised in Fig. 1 and 2, is provided in Fig. 3. As expected, the TEM micrograph from
341 the spinach juice shows a chloroplast structure with visible starch granules, mitochondria,
342 plastoglobules, and stacks of thylakoid membranes called grana (10 – 20 membrane layers) (Fig. 3, SJ).
343 According to Shimoni, Rav-Hon, Ohad, Brumfeld, and Reich (2005) and Wayne (2019), grana have a
344 diameter and thickness of approximately 0.3 and 0.2 - 0.6 µm, respectively. The grana and lamellae
345 structures of the thylakoid membrane can be clearly observed not only in the micrograph taken on SJ
346 but also those taken for in P1 and P2. By contrast, the images for SN1 and SN2 show rounded, vesicle-
347 shaped membrane structures that might have formed from disrupted chloroplasts. Although P1, P2
348 and WBTRF were all pellet samples, some degree of thylakoid membrane disruption (untangling of the
349 stacks) can be observed in the micrograph taken on WBTRF. On the other hand, the micrograph for
350 DP shows an unravelled membrane structure whilst the one for BCRF shows a completely
351 disintegrated membrane system. The latter is undoubtedly due to the high energy input during high
352 pressure homogenisation.

353 Particle size data of different chloroplast materials are shown in Fig. 4. A trimodal distribution
354 was observed for most samples. For instance, filtered SJ (Fig. 4, A) showed minor peaks at 0.2 and
355 101.5 µm, and a major peak at 4.5 µm. The major particle size fraction accounted for 80.0% of the
356 whole population and minor fractions for 4.0 and 16.0%, respectively. The major peak of 4.5 µm
357 compares well to data reported in literature as Möbius described in 1920 (Staehelin, 1986) that an
358 intact chloroplast is approximately 3 – 10 µm in diameter. Here, the value was confirmed by estimating
359 the particle diameter from image analysis, with values of 4.4 ± 0.2, 4.2 ± 0.3 and 5.2 ± 0.2 µm found
360 for CP, BCRF and WBTRF samples, respectively.

361 CP was obtained by centrifugation and the particle size distribution (Fig. 4) indicates a major
362 peak at 5.9 µm (96.2%) and a minor peak at 101.5 µm (3.8%). These values can be attributed to intact
363 chloroplast structures and the presence of debris/cell wall fragments and evidence that the

centrifugation step has successfully isolated intact chloroplasts. The particle size distributions of WBSJ (peak values of 0.2 (~4%), 4.5 (~80%) and 101.5 µm (~16%)) and WBTRF (peak values of 3.9 (~79%) and 59 µm (~21%)) closely resemble the distributions for SJ, DP and CP. However, the TEM micrographs (Fig. 3) reveal a more dispersed membrane system for DP compared to WBSJ and WBTRF. Following high pressure homogenisation (BCRF), the particle size distribution has not unexpectedly shifted to smaller particle sizes with a major peak at 0.2 (~71%) and a minor yet pronounced peak at 2.0 µm (~29%). The microstructures shown in the corresponding TEM micrograph (Fig. 3, BCRF) support the conclusion that high pressure homogenisation has disintegrated the chloroplast membrane structure. Clearly, applying the range of processes considered in this work, summarised in Fig. 1 and 2, allowed to manufacture chloroplast materials with different degrees of integrity.

From Fig. 3 and 4 it can also be seen that the membrane microstructures in the chloroplast/thylakoid samples P1, DP and BCRF were distinctly different, including condensed, untangled and disintegrated membranes, respectively. The microstructure of P2 material closely resembled that of P1 and, thus, they were combined into one overall pellet sample (CP). As a consequence, CP, DP and BCRF were chosen as the materials to be tested in the chocolate model system (65% s/o suspension). All three samples were subjected to freeze-drying. After freeze-drying, CP, DP and BCRF, will be referred to as P-CRF, DP-CRF and B-CRF, respectively. To measure the efficiency of these CMMs' interfacial-active properties, they were tested in the chocolate model system, in comparison to two commercial PGPR samples (PGPR 4150 and G90). Using the method outlined earlier by Lichtenthaler (2001), the total chlorophyll analysis (Chl a and b) was performed. The result indicates that P, DP and B-CRF contain similar amount of Chl ranging from approximately 42 – 48 mg/g DW. Upon applying the chloroplast material in the chocolate model system, depending on the amount of CRF added, the concentration of Chl could varies between 0.021% (in 0.5% w/w sample) to 0.084% (in 2.0% w/w sample).

3.2. Rheological characteristics

The Casson yield point (σ_c), the shear stress at 5 s^{-1} (τ_5), the apparent viscosity (η_{40}), the cross over point (COP) and the tangent flow point (TFP) values determined for the s/o suspensions containing P-CRF, DP-CRF, B-CRF, PGPR 4150, PGRP G90 or no added flow enhancer (control sample) are reported in the Appendix Table A.1. The flow consistency index (η_c) (Chhabra, 1999) (also referred to as viscosity consistency by Pratumwal et al. (2017)) obtained from fitting the Casson model to the experimental data is shown in the Appendix Fig. B.2.

In the literature, multiple models and methods have been used to quantify the yield behaviour of confectionery products (Afoakwa et al., 2009; Rao, 2014). The Casson yield stress, σ_c, is probably the (still) most widely-used yield parameter in the confectionery industry (Rao, 2014). Applying the Casson model to experimental data, initially not necessarily acquired in a prescribed manner, has been the standard method approved by the International Confectionery Association (ICA) in 1973. In an update, the use of pre-shear (5 s^{-1}, ≥ 5 mins) and up and down flow curves (2 – 50 s^{-1}) to create the experimental data for model fitting has been recommended (ICA Method 46) together with a more complex rheological model (Eischen & Windhab, 2002) based on the Windhab equation (Windhab, 1993) and a shear rate correction (Eischen & Windhab, 2002). Nonetheless, the Casson model (Casson, 1959) is still widely used by many researchers (Cahyani et al., 2019; Kumbár, Nedomová, Ondrušíková, & Polcar, 2018) and remains the model of choice for determining the yield stress of chocolate by the National Confectioners Association (NCA) in the United States (formerly Chocolate Manufacturers Association (CMA)) (Baker, Brown, & Anantheswaran, 2006).

The flow point (FP) describes the onset of flow dominated shear deformation. For the s/o suspension systems it was found that determining the FP using oscillatory rheometry (FP_{osc}) is case specific, meaning that the FP_{osc} determination procedure may require a degree of adjustment for different samples. Initially, the suspension containing 0.4% PGPR 4150 was considered. At low oscillatory stress this suspension displayed elastic dominated behaviour where G’ > G’’. With

414 increasing oscillatory stress, the system passed through a cross over point (G' = G'') and at higher
415 stresses viscous dominated behaviour where G'' > G' was exhibited (Fig. 5). For this particular system,
416 two characteristic points can be determined: the tangent flow point and the cross over point. The
417 tangent flow point (TFP) is the crossing of the plateau modulus (i.e., G' Plateau) and the tangent of the
418 decay part of the oscillatory curve (i.e., slope tangent). Technically, it is possible to use the G'' curve
419 to determine another TFP, but this is not widely applied in literature (Dinkgreve, Paredes, Denn, &
420 Bonn, 2016; Malvern Instruments Limited, 2012). The cross over point (COP) is determined as the
421 value of the oscillatory stress where G' = G'', which marks the transition from elastic to viscous
422 dominated deformation. The G' Plateau was plotted using the data points in the region of linear
423 viscoelasticity (i.e., LVE), a range of tests which was carried out without destroying the sample's
424 structure. On the other hands, the slope tangent was plotted using the decay part of the collected G'
425 data. Both of these tangent lines can be use together to approximate the point of phase transition in
426 the sample. For the suspension with the higher amount of PGPR 4150 (0.6%), it can be seen that the
427 value for the Casson yield stress is almost negligible (Appendix Table A.1). However, a TFP could still
428 be determined although a COP does not exist since viscous dominated behaviour (G'' > G') prevailed
429 throughout the range of oscillatory stresses applied. Yet another type of behaviour was observed for
430 the 0% PGPR sample, a discontinuity point. For stress values below the discontinuity point, the
431 sample's LVE behaviour was elastic dominated, whilst for oscillatory stresses above the discontinuity
432 point onset of flow was observed (G'' > G'). In such case, the TFP and COP points cannot be
433 distinguished and both coincide with the discontinuity point, which was taken as the flow point for
434 this type of system (Fig. 5).

435 Fig. 6 illustrates the flow curves for the formulated s/o suspensions across the range of
436 emulsifier systems and concentration applied, including the control sample (no emulsifier added). For
437 all samples, it was possible to identify a region of the flow curve that can be described as a high shear
438 plateau where the change in viscosity with shear stress is negligible. With decreasing shear stress, the

systems approached the yield point that sees a steep rise of the viscosity values. Fig. 6A shows the flow curves for s/o suspensions containing PGPR 4150 or G90. At any given concentration applied PGPR 4150 is more efficient in reducing yield stress than PGPR G90, which is reflected in the Casson yield stress values shown in Fig. 7 and aligns with recently published Herschel-Bulkley yield stress values for these PGPR products (Price et al., 2022).

Fig. 6B shows the flow curves for suspensions containing freeze-dried chloroplast samples P-CRF, DP-CRF or B-CRF. They resemble in shape those of suspensions containing PGPR (Fig. 6A). The capacity of the B-CRF material to reduce the yield was markedly lower than of P-CRF and DP-CRF. Fig. 6C offers a direct comparison of the yield stress reducing behaviour of the best performing chloroplast material P-CRF with the better (of the two) performing PGPR 4150.

Using the Casson equation (Eq. 1) and flow curve data, σ_c, η_c, τ_5 and η_{40} can be calculated. The dependencies of the calculated rheological parameters on emulsifier type and concentration are shown in Fig. 7 (the data for η_c are provided in Appendix Fig. B.2). Comparing σ_c and τ_5 of all samples reveals that PGPR 4150 is the most effective emulsifier due to its lower yield stresses values. This is closely followed by PGPR G90, DP-CRF, P-CRF and B-CRF respectively. The σ_c and τ_5 values for the control sample (no emulsifier) are found to be 63.5 ± 19.5 and 185.8 ± 34.2 Pa, respectively. Addition of 0.1% of PGPR 4150 resulted in a decrease of σ_c and τ_5 by 93.2% (4.3 $\pm$ 2.0 Pa) and 83.7% (30.3 $\pm$ 7.6 Pa), respectively. PGPR G90, however, reduced σ_c only by 51.8% (30.6 $\pm$ 4.1 Pa) and τ_5 by 60.2% (74.0 $\pm$ 8.3 Pa).

Although less effective than PGPR, the three chloroplast/thylakoid materials tested (P-CRF, DP-CRF and B-CRF) clearly demonstrated a strong ability to reduce the yield value of the highly concentrated s/o suspension, acting as a chocolate model system. At 1.0%, DP-CRF performed slightly better than P-CRF and B-CRF, reducing σ_c and τ_5 to 2.0 $\pm$ 0.3 and 26.9 $\pm$ 1.7 Pa, respectively. 1.0% P-CRF and B-CRF both lead to significantly higher values of σ_c and τ_5; P-CRF: 5.37 ± 2.36 and 39.68 ± 6.82 Pa; B-CRF: 6.02 ± 1.56 and 40.04 ± 5.07 Pa, respectively. Further increase in the concentration of

any of the chloroplast/thylakoid materials (2.0% and 3.0%) resulted in a diminishing emulsifier effectiveness. According to Figure 7, the σ_C data illustrates that the efficiency of chloroplast/thylakoid material in aiding flowability in the chocolate model system decreased from DP-CRF to P-CRF to B-CRF. This phenomenon is marked by 1.0 and 2.0% concentration of the chloroplast material. It was hypothesised that the emulsifying ability of CRF material is correlated to the galactolipids content in each sample. From the analysis, the galactolipids (i.e., MGDG and DGDG) concentration is highest in DP and P-CRF sample with approximately 42 – 33 µg/g DW. In B-CRF, however, the galactolipids fall to about 17 µg/g DW. This observation supports the result seen from the unidirectional and oscillatory measurements.

The oscillatory rheology data were used to determine the tangent flow point (TFP) and the cross over point (COP). As aforementioned, for samples showing modulus discontinuity, TFP and COP coincided (TFP = COP). The dependency of TFP and COP on emulsifier type and concentration is shown in Fig. 8 and it mirrors that of σ_c and τ_5. The COP of the control sample (no emulsifier) was 6.6 ± 0.7 Pa. An addition of 0.2% PGPR 4150 resulted in the COP decreasing to 1.5 ± 0.4 Pa. This value is comparable to those found for the addition of 1.0% DP-CRF (1.4 ± 0.2 Pa), P-CRF (1.6 ± 0.3 Pa) or B-CRF (1.8 ± 0.2 Pa).

With an increase in emulsifier concentration, the flow behaviour transitioned from an elastic (G' > G'') to viscous (G'' > G') domination (Fig. 5). Progressively, the s/o suspension required less energy to initiate flowing and as such, the COP gradually moved to lower oscillatory stresses. In the case of 0.6% PGPR 4150, the COP even moved outside the range of oscillatory shear stress values applied with G'' > G' throughout (Fig. 5). Conversely, the value for η_c approached 1 as shown in Appendix Fig. B.2. However, the TFP could still be determined using the extrapolation method (0.10 ± 0.01 Pa).

Although the main purpose of formulating PGPR into confectionery products is to reduce the yield stress, it concurrently reduces the apparent viscosity (Beckett, 2009). PGPR was observed to reduce η_{40} of the control (15.4 ± 1.7 Pa s) to 2.6 ± 0.2 and 2.3 ± 0.3 Pa s upon addition of 0.2% PGPR

G90 and 4150, respectively. Similar to σ_c and τ_5, no significant differences were observed between adding 0.2% PGPR G90 and 1.0% DP-CRF material.

3.3. Suspension Microstructure

To gain insight into the interaction between the chloroplast/thylakoid materials and sugar particles suspended in oil, the microstructure of a s/o suspension containing P-CRF was visualised using confocal laser scanning microscopy. More precisely, 1.0% Rhodamine B-stained P-CRF (S-CRF) was applied in a s/o suspension with the reduced sugar content of 50% (w/w) which benefitted image quality. Rhodamine B is a protein-specific stain and targets the integral and peripheral proteins embedded within the chloroplast membrane structures (outer-, inner-envelope and thylakoid membranes). Since sugar and sunflower oil contain no protein, the features in Fig. 9 identify the presence of proteins, which, in turn, indicates the presence of complex membrane systems. Fig. 9 illustrates the maximum intensity projection while Appendix Fig. C.3 provides micrographs obtained at four different planes: Z = 1 - 4.

As seen on the micrograph of plane 1 (Z = 1) (Appendix Fig. C.3A), a large amount of membrane structure surrounded the sugar particles ($d_{4,3}$ = 35.6 ± 2.3 µm, Appendix Fig. A.1) suspended in the system. Each z-plane had a thickness difference of 0.2 – 0.5 µm and the micrographs (Appendix Fig. C.3B, C and D) display the membrane structure located on the upper surface of the sugar particles. Together, these micrographs show the image of protein-stained membranes material enveloping the sugar particles on different planes. Overall, the confocal micrographs demonstrate the adsorption of chloroplast/thylakoid membrane structures onto the sugar particles suspended in the system. Rounded, bright red structures can also be observed in the micrograph, indicating freely suspended fragments of S-CRF material.

Thylakoid membranes have been reported to stabilise oil-in-water emulsions by encompassing the oil droplets and acting as barriers preventing coalescence (Rayner, Ljusberg, et al., 2011). Such barrier properties (Rayner, Ljusberg, et al., 2011) offer a potential explanation for the behaviour of chloroplast material in an oil-based suspension, similar to the mechanism proposed for PGPR. PGPR molecules were observed to form pillow-like structures surrounding sugar particles suspended in oil, acting as a barrier preventing these lipophobic particles to aggregate thus enhancing the flow of the suspension (Middendorf, Juadjur, Bindrich, & Mischnick, 2015). Similarly, the presence of chloroplast particulates at the surface of sugar particles may create a repulsive barrier that prevents sugar particle agglomeration, resulting in the enhanced flowability revealed in this work.

4. Conclusion

Overall, it is possible, using physical methods, to prepare chloroplast membranes displaying a range of disorder. Unidirectional and oscillatory measurements showed that the addition of emulsifiers (PGPR [4150 & G90] & chloroplast/thylakoid materials [P-CRF, DP-CRF & B-CRF]) reduced the energy required to initiate the flow of the s/o suspension. Progressive addition of chloroplast-based emulsifier material resulted in the reduction of the yield stress measures (τ_5 and σ_c), apparent viscosity (η_{40}), and COP and TFP values. An increase of the concentration of chloroplast/thylakoid materials above 2.0% resulted in diminishing effectiveness. The ultimate effectiveness of these material was comparable with 0.2% PGPR. By analysing confocal laser scanning micrographs of the chloroplast/thylakoid materials there was evidence of chloroplast membranes surrounding sugar particles. Assuming the membranes remained intact, as observed in TEM, then we are observing an interaction between a multicomponent membrane at the surface of sugar particles. There is, however, the possibility that the lipid elements of the membrane gradually partition into the oil phase. Given

that a commercial process to produce chloroplast material is likely to include a stage to knock out endogenous enzymes to stabilise the material, it would of interest to test the impact of heat-treatment on the properties of the chloroplast membranes.

Overall, this study introduces a simple physical method to prepare interfacial-active chloroplast membrane material, without the need to perform any lipid extraction involving the use of organic solvents. As confectionery formulations often involve PGPR (Mahamad, 2017; Peker et al., 2013; Schantz & Rohm, 2005), these materials hold strong potential as nutrient-rich alternatives to chemical and synthetic flow enhancer in chocolate manufacture.

Acknowledgements

The research published was conducted as a part of a PhD in Food Science at the University of Nottingham. PS would like to convey their sincere gratitude toward Denise Mclean and Ian Ward for their assistance in obtaining transmission electron and confocal micrographs, respectively.

552 **References**

553 Afoakwa, E. O. (2016). Cocoa processing technology. In *Chocolate Science and Technology* (pp. 102-
554 116).

555 Afoakwa, E. O., Paterson, A., & Fowler, M. (2007). Factors influencing rheological and textural
556 qualities in chocolate – a review. *Trends in Food Science & Technology, 18*(6), 290-298.
557 doi:https://doi.org/10.1016/j.tifs.2007.02.002

558 Afoakwa, E. O., Paterson, A., Fowler, M., & Vieira, J. (2009). Comparison of rheological models for
559 determining dark chocolate viscosity. *International Journal of Food Science & Technology,*
560 *44*(1), 162-167. doi:https://doi.org/10.1111/j.1365-2621.2008.01710.x

561 Albertsson, P. A., Kohnke, R., Emek, S. C., Mei, J., Rehfeld, J. F., Akerlund, H. E., & Erlanson-
562 Albertsson, C. (2007). Chloroplast membranes retard fat digestion and induce satiety: effect
563 of biological membranes on pancreatic lipase/co-lipase. *Biochem J, 401*(3), 727-733.
564 doi:10.1042/BJ20061463

565 Baker, B., Brown, B., & Anantheswaran, R. (2006). Measurement of yield stress in dark chocolate
566 using controlled stress vane method. *Journal of Texture Studies, 37*, 655-667.
567 doi:10.1111/j.1745-4603.2006.00076.x

568 Beckett, S. T. (2009). *The Science of Chocolate* (2nd ed.). Cambridge, United Kingdom: The Royal
569 Society of Chemistry.

570 Block, M. A., Dorne, A. J., Joyard, J., & Douce, R. (1983). Preparation and Characterization of
571 Membrane Fractions Enriched in Outer and Inner Envelope Membranes from Spinach
572 Chloroplasts. *The Journal of Biological Chemistry, 258*(21), 13281 - 13286.

573 Cahyani, A., Kurniasari, J., Nafingah, R., Rahayoe, S., Harmayani, E., & Saputro, A. D. (2019).
574 Determining casson yield value, casson viscosity and thixotropy of molten Chocolate using
575 viscometer. *IOP Conference Series: Earth and Environmental Science, 355*(1), 012041.
576 doi:10.1088/1755-1315/355/1/012041

577 Casson, N. (1959). *A Flow Equation for Pigment-oil Suspensions of the Printing Ink Type. Reprinted*
578 *from "Rheology of Disperse Systems."*.

579 Chhabra, R. P. (1999). *Non-Newtonian flow in the process industries : fundamentals and engineering*
580 *applications / R.P. Chhabra and J.F. Richardson*. Oxford: Oxford : Butterworth-Heinemann.

581 De Graef, V., Depypere, F., Minnaert, M., & Dewettinck, K. (2011). Chocolate yield stress as
582 measured by oscillatory rheology. *Food Research International, 44*(9), 2660-2665.
583 doi:10.1016/j.foodres.2011.05.009

584 Dinkgreve, M., Paredes, J., Denn, M. M., & Bonn, D. (2016). On different ways of measuring “the”
585 yield stress. *Journal of Non-Newtonian Fluid Mechanics, 238*, 233-241.
586 doi:https://doi.org/10.1016/j.jnnfm.2016.11.001

587 EFSA Panel on Food Additives Nutrient Sources added to Food, Mortensen, A., Aguilar, F., Crebelli,
588 R., Di Domenico, A., Dusemund, B., . . . Lambré, C. (2017). Re-evaluation of polyglycerol
589 polyricinoleate (E 476) as a food additive. *EFSA Journal, 15*(3), e04743.
590 doi:https://doi.org/10.2903/j.efsa.2017.4743

Eischen, J.-C., & Windhab, E. J. (2002). Viscosity of Cocoa and Chocolate Products. *Applied Rheology, 12*(1), 32-34. doi:doi:10.1515/arh-2002-0020

Gedi, M. A., Briars, R., Yuseli, F., Zainol, N., Darwish, R., Salter, A. M., & Gray, D. A. (2017). Component analysis of nutritionally rich chloroplasts: recovery from conventional and unconventional green plant species. *Journal of Food Science and Technology, 54*(9), 2746-2757. doi:10.1007/s13197-017-2711-8

Gedi, M. A., Magee, K. J., Darwish, R., Eakpetch, P., Young, I., & Gray, D. A. (2019). Impact of the partial replacement of fish meal with a chloroplast rich fraction on the growth and selected nutrient profile of zebrafish (Danio rerio). *Food Funct, 10*(2), 733-745. doi:10.1039/c8fo02109k

Kumbár, V., Nedomová, Š., Ondrušíková, S., & Polcar, A. (2018). Rheological behaviour of chocolate at different temperatures. *Potravinarstvo Slovak Journal of Food Sciences, 12*, 123-128. doi:10.5219/876

Lichtenthaler, H., K., Buschmann, C. (2001). Chlorophylls and Carotenoids: Measurement and Characterization by UV-Vis Spectroscopy *Current Protocols in Food Analytical Chemistry 1*(1), F4.3.1 - F4.3.8. doi: https://doi.org/10.1002/0471142913.faf0403s01

Mahamad, N. J. (2017). *Dark Chocolate: Understanding The Impact of Limonene on the Crystallization Properties and Application of Green Leaf Lipid Extract as a Flow Enhancer* (PhD). University of Nottingham

Malvern Instruments Limited. (2012). *Understanding Yield Stress Measurements*. Retrieved from

Manasi, I., Arnold, T., Cooper, J. F. K., Van Damme, I., Dong, C., Saerbeck, T., . . . Titmuss, S. (2019). Planar sucrose substrates for investigating interfaces found in molten chocolate. *Food Structure, 22*, 100128. doi:10.1016/j.foostr.2019.100128

Middendorf, D., Juadjur, A., Bindrich, U., & Mischnick, P. (2015). AFM approach to study the function of PGPR's emulsifying properties in cocoa butter based suspensions. *Food Structure, 4*, 16-26. doi:https://doi.org/10.1016/j.foostr.2014.11.003

Food Additives in Europe 2000 - Status of safety assessments of food additives presently permitted in the EU (2002).

Mohamad, N. J., Gray, D., & Wolf, B. (2020). Spinach leaf and chloroplast lipid: A natural rheology modifier for chocolate? *Food Research International, 133*, 109193. doi:https://doi.org/10.1016/j.foodres.2020.109193

Osborn, S. (2015). 12 - Labelling relating to natural ingredients and additives. In P. Berryman (Ed.), *Advances in Food and Beverage Labelling* (pp. 207-221). Oxford: Woodhead Publishing.

Ostbring, K., Sjoholm, I., Sorenson, H., Ekholm, A., Erlanson-Albertsson, C., & Rayner, M. (2018). Characteristics and functionality of appetite-reducing thylakoid powders produced by three different drying processes. *J Sci Food Agric, 98*(4), 1554-1565. doi:10.1002/jsfa.8627

Peker, B. B., Suna, S., Tamer, C. E., & Copur, O. U. (2013). The Effect of Lecithin and Polyglycerol Polyricinoleate (PGPR) on Quality of Milk, Bitter and White Chocolates *Journal of Agricultural Faculty of Uludag University*, 1-16.

Pratumwal, Y., Limtrakarn, W., Muengtaweepongsa, S., Phakdeesan, P., Duangburong, S., Eiamaram, P., & Intharakham, K. (2017). Whole blood viscosity modeling using power law, Casson, and Carreau Yasuda models integrated with image scanning U-tube viscometer technique. *Songklanakarin Journal of Science and Technology, 39*, 625-631. doi:10.14456/sjst-psu.2017.77

Price, R., Gray, D., Watson, N., Vieira, J., & Wolf, B. (2022). Linking the yield stress functionality of polyglycerol polyricinoleate in a highly filled suspension to its molecular properties. *LWT, 165*, 113704. doi:https://doi.org/10.1016/j.lwt.2022.113704

Quest International. (1997). *Summary of Legislative Approvals for Polyglycerol Polyricinoleate (PGPR) Admul WOL TM*. Retrieved from

Rao, M. A. (2014). Flow and Functional Models for Rheological Properties of Fluid Foods. 27-61. doi:10.1007/978-1-4614-9230-6_2

Rayner, M., Emek, S. C., Gustafssona, K., Albertsson, C. E., & Albertsson, P.-Å. (2011). A novel emulsifier from spinach with appetite regulation abilities. *Procedia Food Science, 1*, 1431-1438. doi:10.1016/j.profoo.2011.09.212

Rayner, M., Ljusberg, H., Emek, S. C., Sellman, E., Erlanson-Albertsson, C., & Albertsson, P.-Å. (2011). Chloroplast thylakoid membrane-stabilised emulsions. *Journal of the Science of Food and Agriculture, 91*(2), 315-321. doi:10.1002/jsfa.4187

Schantz, B., & Rohm, H. (2005). Influence of lecithin–PGPR blends on the rheological properties of chocolate. *LWT - Food Science and Technology, 38*(1), 41-45. doi:10.1016/j.lwt.2004.03.014

Schindelin, J., Arganda-Carreras, I., Frise, E., Kaynig, V., Longair, M., Pietzsch, T., . . . Cardona, A. (2012). Fiji: an open-source platform for biological-image analysis. *Nature Methods, 9*(7), 676-682. doi:10.1038/nmeth.2019

Servais, C., Ranc, H., & Roberts, I. D. (2003). DETERMINATION OF CHOCOLATE VISCOSITY. *Journal of Texture Studies, 34*(5-6), 467-497. doi:https://doi.org/10.1111/j.1745-4603.2003.tb01077.x

Shafi, F., Reshi, M., Aiman, & Bashir, I. (2018). Chocolate Processing *International Journal of Advanced Biological Research 8*(3), 408 - 419.

Shimoni, E., Rav-Hon, O., Ohad, I., Brumfeld, V., & Reich, Z. (2005). Three-dimensional organization of higher-plant chloroplast thylakoid membranes revealed by electron tomography. *Plant Cell, 17*(9), 2580-2586. doi:10.1105/tpc.105.035030

Sözeri Atik, D., Bölük, E., Toker, O. S., Palabiyik, I., & Konar, N. (2020). Investigating the effects of Lecithin-PGPR mixture on physical properties of milk chocolate. *LWT, 129*, 109548. doi:https://doi.org/10.1016/j.lwt.2020.109548

Staehelin, L. A. (1986). *Chloroplast Structure and Supramolecular Organization of Photosynthesis Membranes* (Vol. 19). Germany Springer-Verlag.

Syamila, M., Gedi, M. A., Briars, R., Ayed, C., & Gray, D. A. (2019). Effect of temperature, oxygen and light on the degradation of beta-carotene, lutein and alpha-tocopherol in spray-dried spinach juice powder during storage. *Food Chem, 284*, 188-197. doi:10.1016/j.foodchem.2019.01.055

669 Tenorio, A. T., de Jong, E. W., Nikiforidis, C. V., Boom, R. M., & van der Goot, A. J. (2017). Interfacial
670 properties and emulsification performance of thylakoid membrane fragments. *Soft Matter,*
671 *13*(3), 608-618. doi:10.1039/c6sm02195f

672 Torcello-Gomez, A., Gedi, M. A., Ibbett, R., Nawaz Husain, K., Briars, R., & Gray, D. (2019).
673 Chloroplast-rich material from the physical fractionation of pea vine (Pisum sativum)
674 postharvest field residue (Haulm). *Food Chem, 272*, 18-25.
675 doi:10.1016/j.foodchem.2018.08.018

676 Wattanakul, J., Sahaka Mahaman Salah, M. B., Amara Ep Douzi, S., Syamila, M., Gontero, B., Carrière,
677 F., & Gray, D. (2019). In vitro digestion of galactolipids from chloroplast-rich fraction (CRF) of
678 postharvest, pea vine field residue (haulm) and spinach leaves. *Food & Function, 10*.
679 doi:10.1039/C9FO01867K

680 Wattanakul, J., Syamila, M., Briars, R., Ayed, C., Price, R., Darwish, R., . . . Gray, D. A. (2021). Effect of
681 steam sterilisation on lipophilic nutrient stability in a chloroplast-rich fraction (CRF)
682 recovered from postharvest, pea vine field residue (haulm). *Food Chem, 334*, 127589.
683 doi:10.1016/j.foodchem.2020.127589

684 Wattanakul, J., Syamila, M., Darwish, R., Gedi, M. A., Sutcharit, P., Chi, C., . . . Gray, D. A. (2022).
685 Bioaccessibility of essential lipophilic nutrients in a chloroplast-rich fraction (CRF) from
686 agricultural green waste during simulated human gastrointestinal tract digestion. *Food &*
687 *Function, 13*(9), 5365-5380. doi:10.1039/D2FO00604A

688 Wayne, R. (2019). *Chloroplasts*: Elsevier Science Publishing Co Inc.

689 Wilson, R., Van Schie, B. J., & Howes, D. (1998). Overview of the preparation, use and biological
690 studies on polyglycerol polyricinoleate (PGPR). *Food Chem Toxicol, 36*(9-10), 711-718.
691 doi:10.1016/s0278-6915(98)00057-x

692 Windhab, E. (1993). Bericht: IV. *Tagung Lebensmittel rheologie detmold*.

693 Wolf, F., Koehler, K., & Schuchmann, H. P. (2013). Stabilization of Water Droplets in Oil with PGPR for
694 Use in Oral and Dermal Applications. *Journal of Food Process Engineering, 36*(3), 276-283.
695 doi:https://doi.org/10.1111/j.1745-4530.2012.00688.x

696

Corresponding Figures

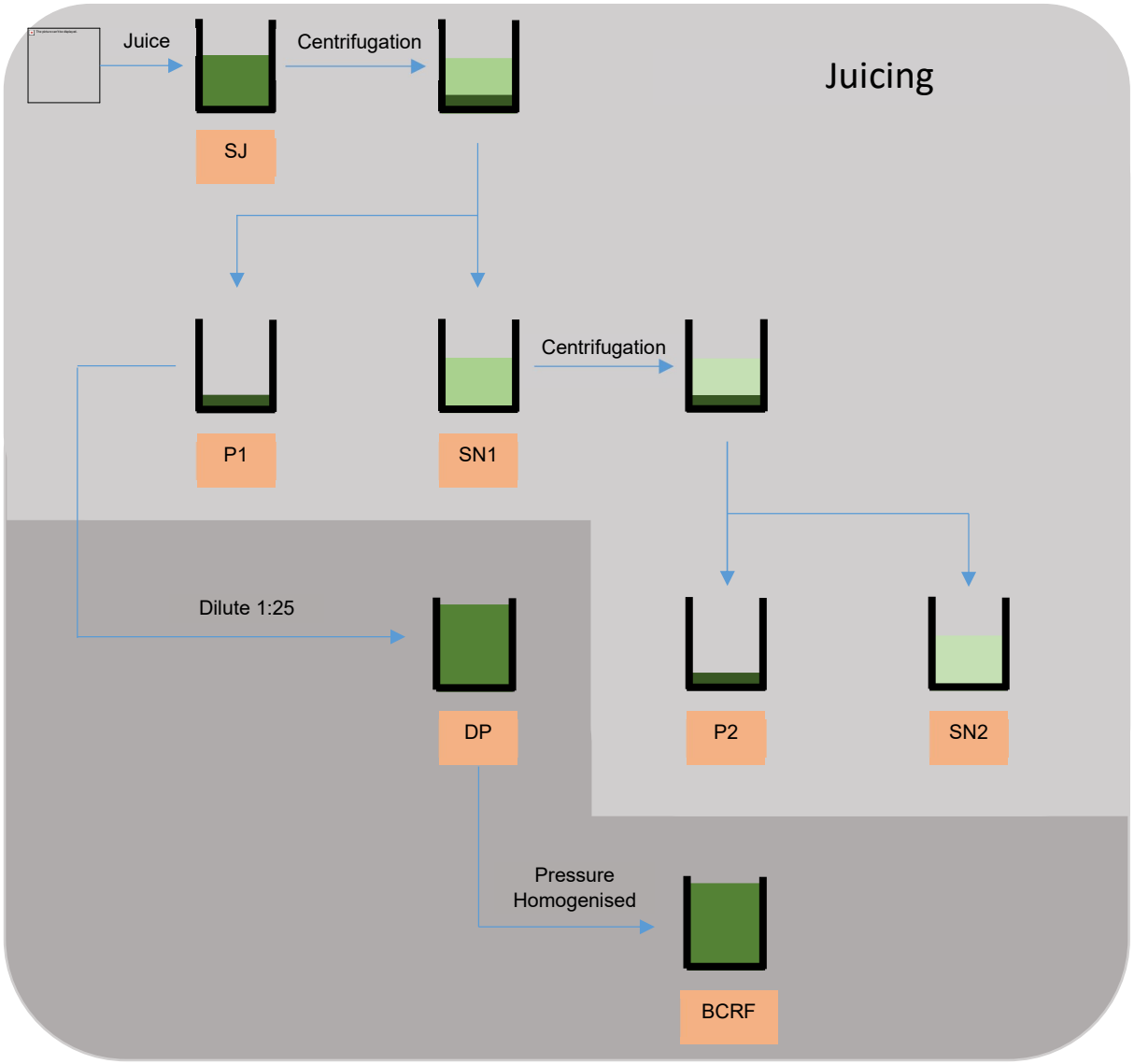

Figure 1: Simplified flow chart for the preparation of largely intact chloroplast (P1 and P2), untangled chloroplast membrane (diluted pellet, DP) and burst chloroplast-rich fraction (BCRF) via juicing from spinach leaves. SJ: spinach juice, P1 and SN1: pellet and supernatant respectively from centrifuged SJ, P2 and SN2: pellet and supernatant respectively from centrifuged SN1.

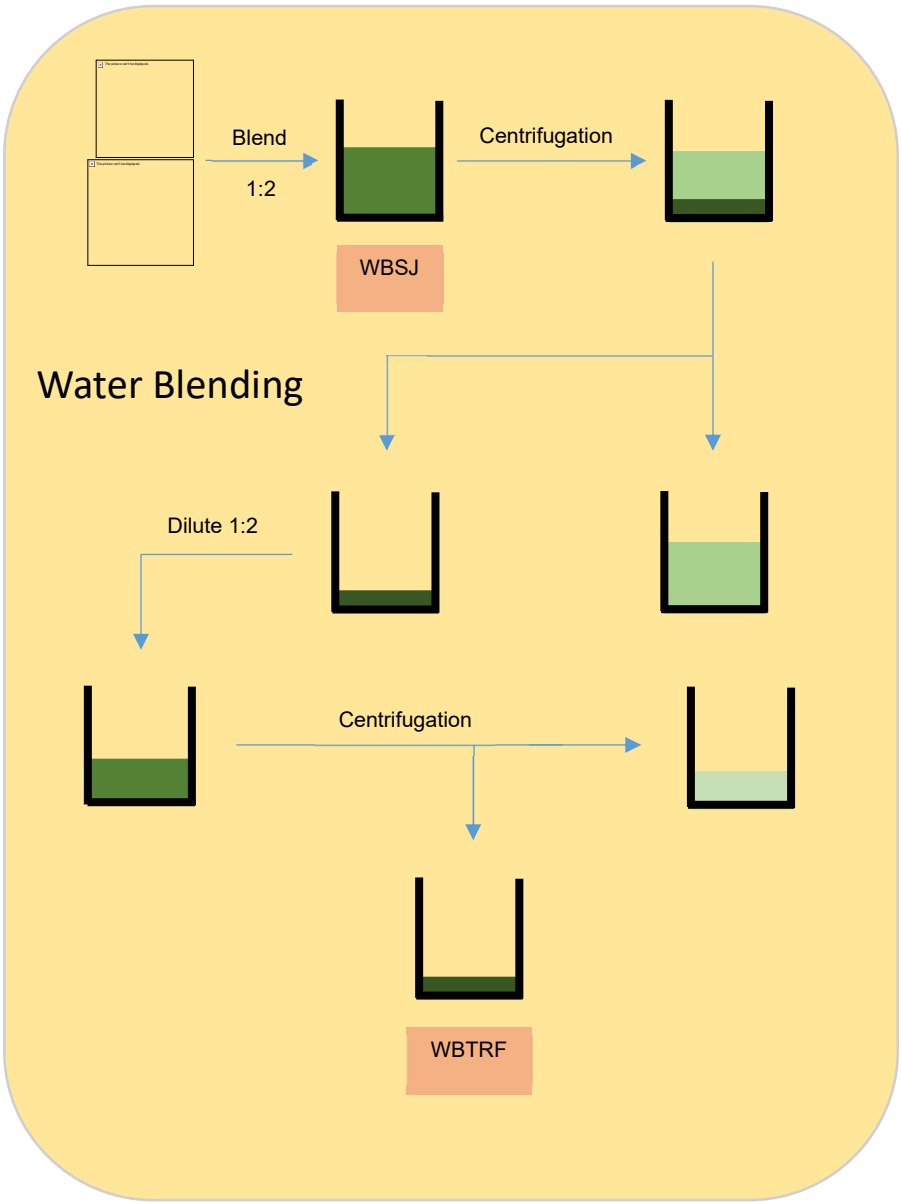

704

705

706 **Figure 2:** Simplified flow chart for the preparation of water-blended thylakoid-rich fraction (WBTRF)

707 from water-blended spinach juice (WBSJ).

708

709

710

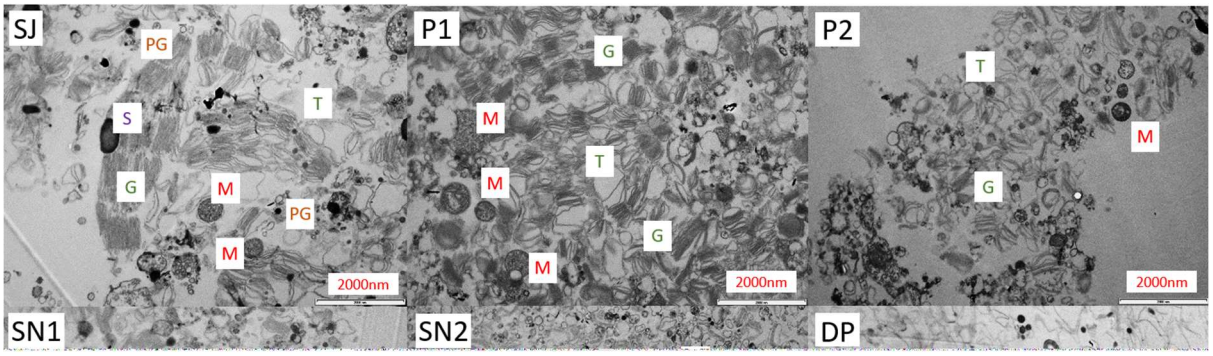

711

712 **Figure 3:** Transmitted electron micrographs of chloroplast materials taken at X9900 magnification. The
713 samples are as follow: spinach juice (SJ), pellet 1 (P1), pellet 2 (P2), supernatant 1 (SN1), supernatant
714 2 (SN2), dilute spinach juice (DP), burst-chloroplast-rich fraction (BCRF), water blended spinach juice
715 (WBSJ) and water blended thylakoid-rich fraction (WBTRF). Structures labelled include: Starch (S),
716 Mitochondria (M), Thylakoid (T), Grana (G), and Plastoglobule (PG). All scale bars correspond to 2000
717 nm.

718

719

720

721

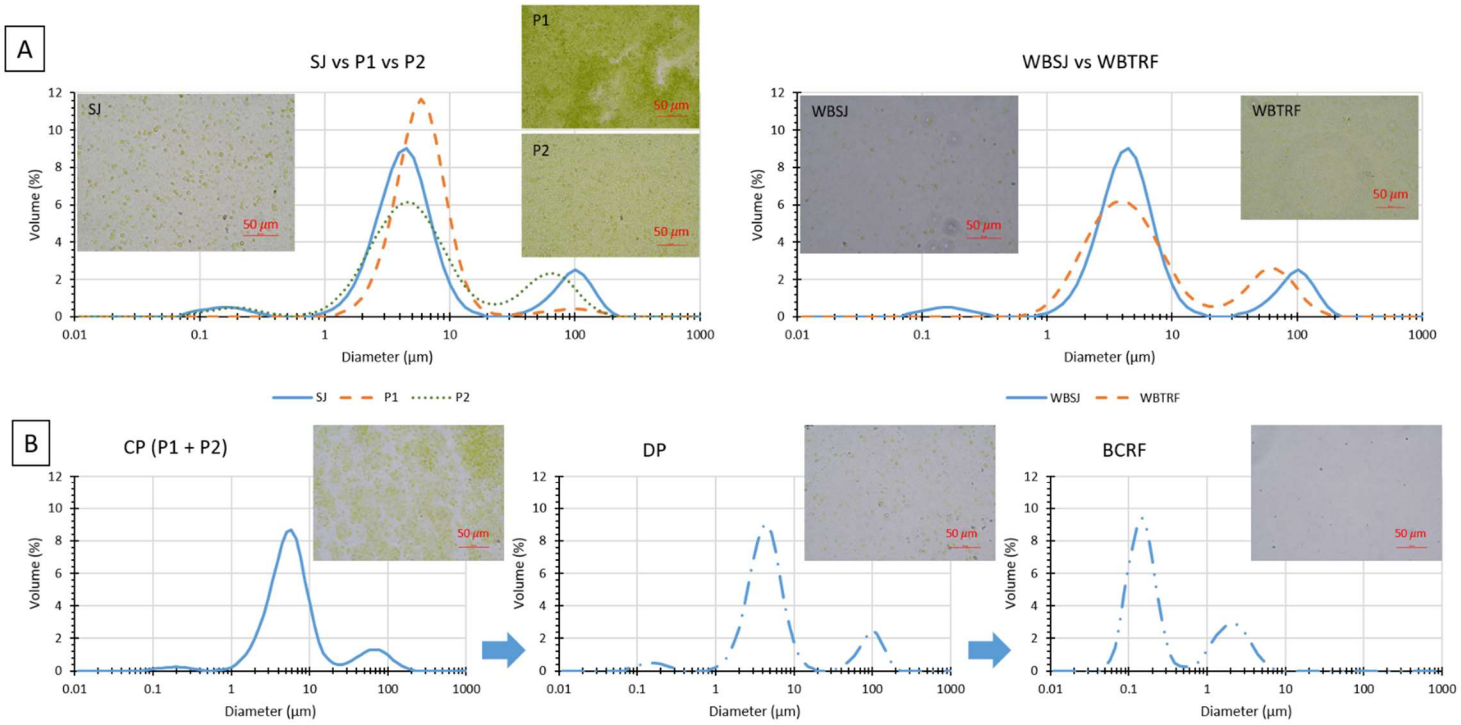

Figure 4: Particle size distribution and corresponding transmission light micrographs of chloroplast/thylakoid samples prepared from juicing and blending method. (A) The left-hand panel shows the effect of sequential centrifugation on the particle size profile of spinach juice sample obtained from extrusion (SJ) and the right-hand panel the water-blended spinach juice (WBSJ) (Smooth line). The pellet samples from juicing method are pellet 1 (P1) (Dashed line) and pellet 2 (P2) (Dotted line), while water blended thylakoid-rich fraction (WBTRF) (Dashed line) represents the pellet sample after centrifugation of the sample obtained from WB-method. In (B), the effect of dilution and pressure homogenization on the overall pellet sample (P1 + P2) particle size is illustrated. All transmission light micrographs were obtained at 400X total magnification, and all scale bars correspond to 50 µm.

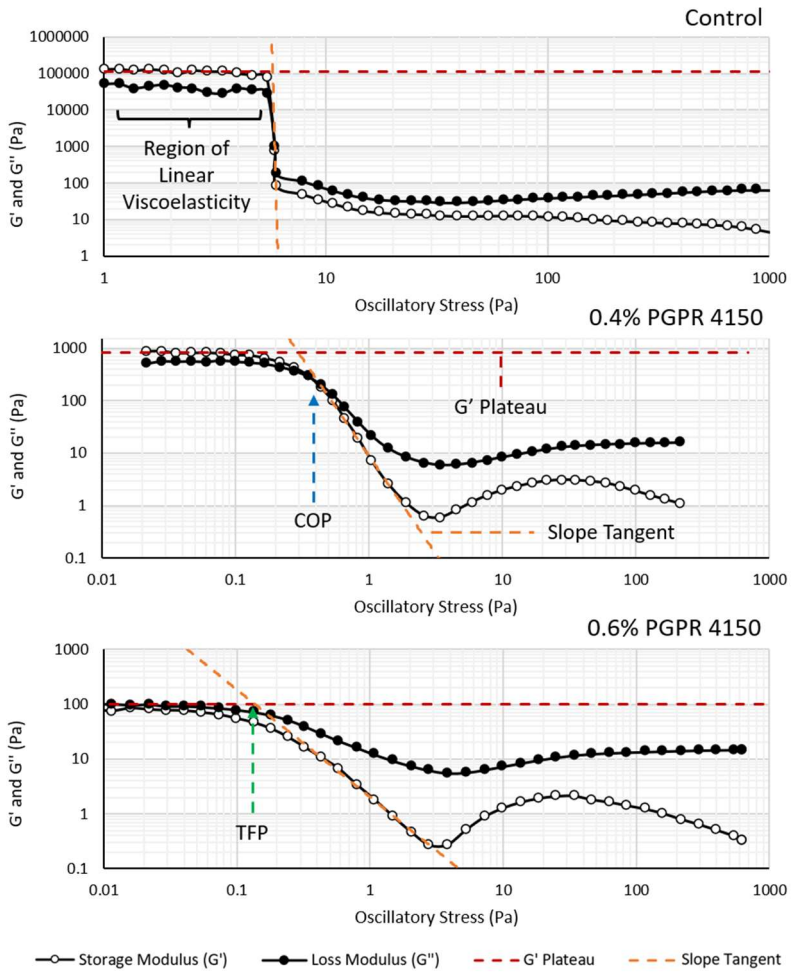

Figure 5: Determination of tangent flow point (TFP) from oscillatory measurements: Control (A), 0.4% PGPR 4150 (B) and 0.6% PGPR 4150 (C). The red and yellow dashed lines represent the tangent lines plotted using data points from the region of linear viscoelasticity (i.e., G' Plateau) and the decaying portion of G' data (i.e., slope tangent), respectively. The cross over between the G' and G'' lines is referred to as the cross over point (COP) while the cross between the tangent lines, the TFP. At 0% PGPR (control), a discontinuity point is observed. For the stress values below the discontinuity point, the sample display an elasticity dominated behaviour (G' > G'') while for the stress values above the discontinuity point the sample display a viscosity dominated behaviour (G'' > G'). In this case, the TFP and cross over point (COP) coincided.

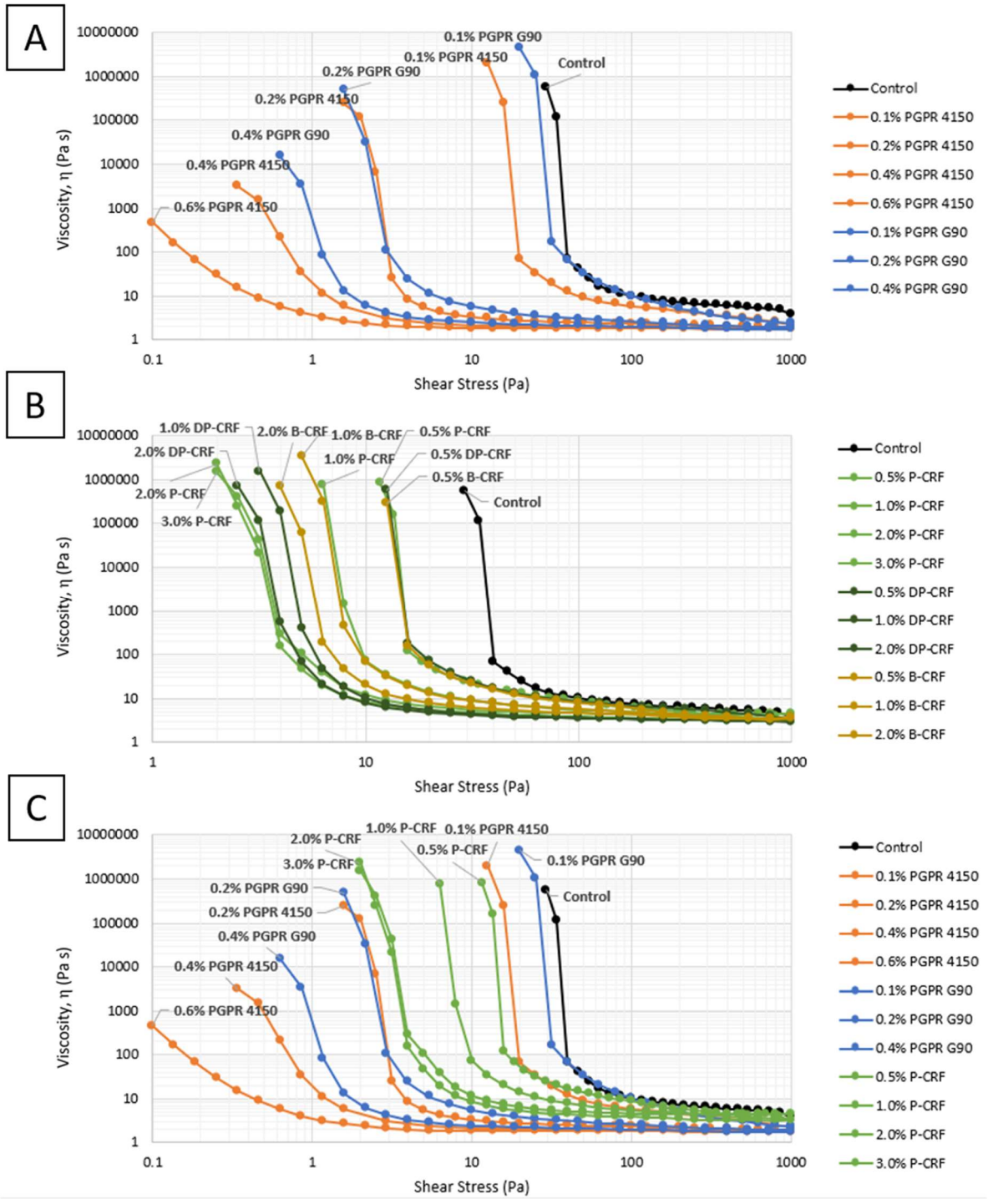

747

748 **Figure 6:** Flow curves obtained from unidirectional measurements following a ramp-down protocol
749 (1,000 Pa to 0.01 Pa). (A) Suspensions containing PGPR 4150 or PGPR G90, and control. (B) Suspensions
750 containing any of the three chloroplast/thylakoid materials P-CRF, DP-CRF or B-CRF, and control. (C)
751 Suspensions containing PGPR 4150 or PGPR G90 or P-CRF material, and control.

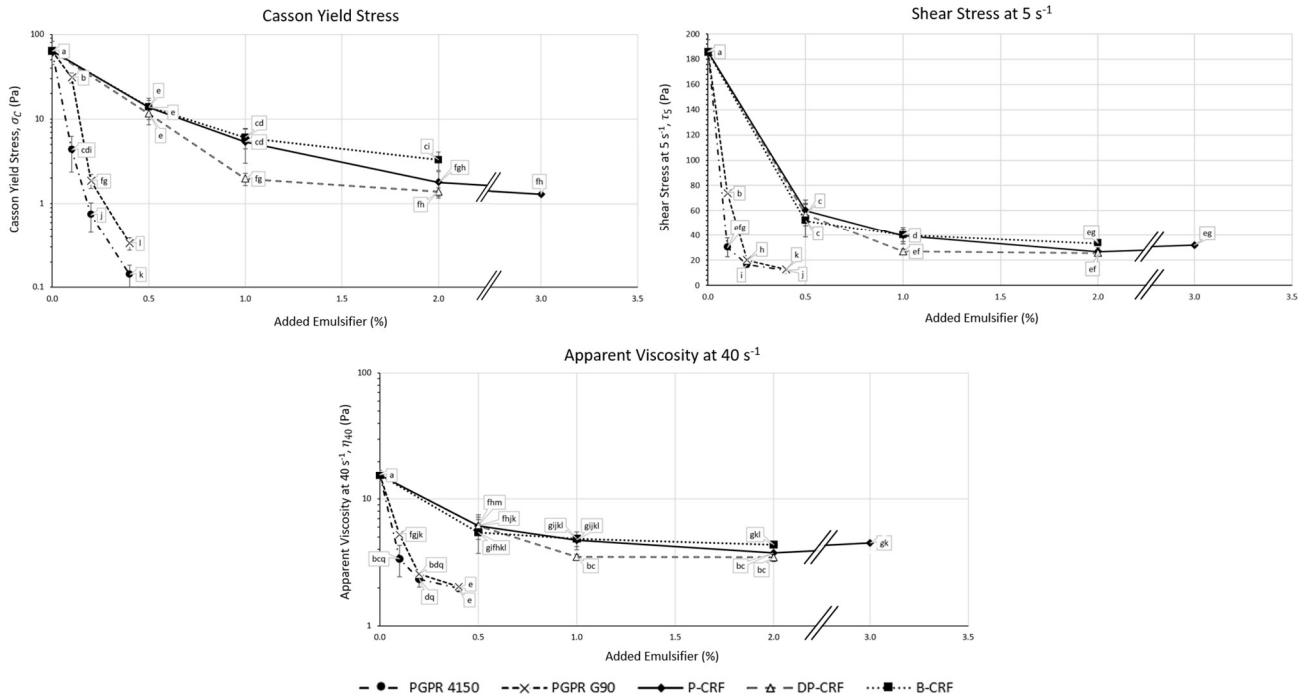

752

753 **Figure 7:** A reduction in Casson yield stress (σ_C), shear stress at 5 s^{-1} (τ_5) and apparent viscosity (η_{40})
754 obtained from unidirectional experiments. The statistical differences are denoted by lowercase
755 letters.

756

757

758

759

760

761

762

763

764

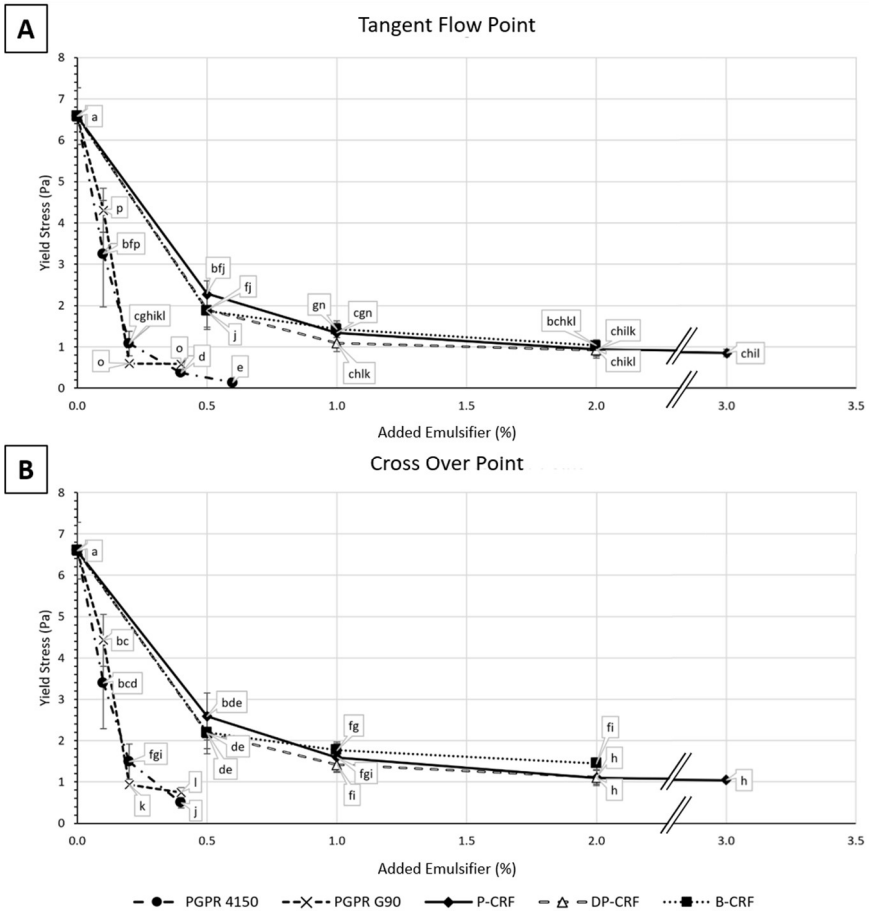

765

766 **Figure 8:** A reduction in Tangent Flow Point (TFP) and Cross Over Point (COP) obtained from oscillatory
767 rheological experiments. The statistical analysis for all data is represented with lowercase letters. For
768 0.6% PGPR 4150, the sample displayed a viscosity dominated behaviour (G'' > G') throughout the
769 tested range. As such, 0.6% PGPR 4150 do not possess a COP but the value for TFP can be determined
770 via extrapolation.

771

772

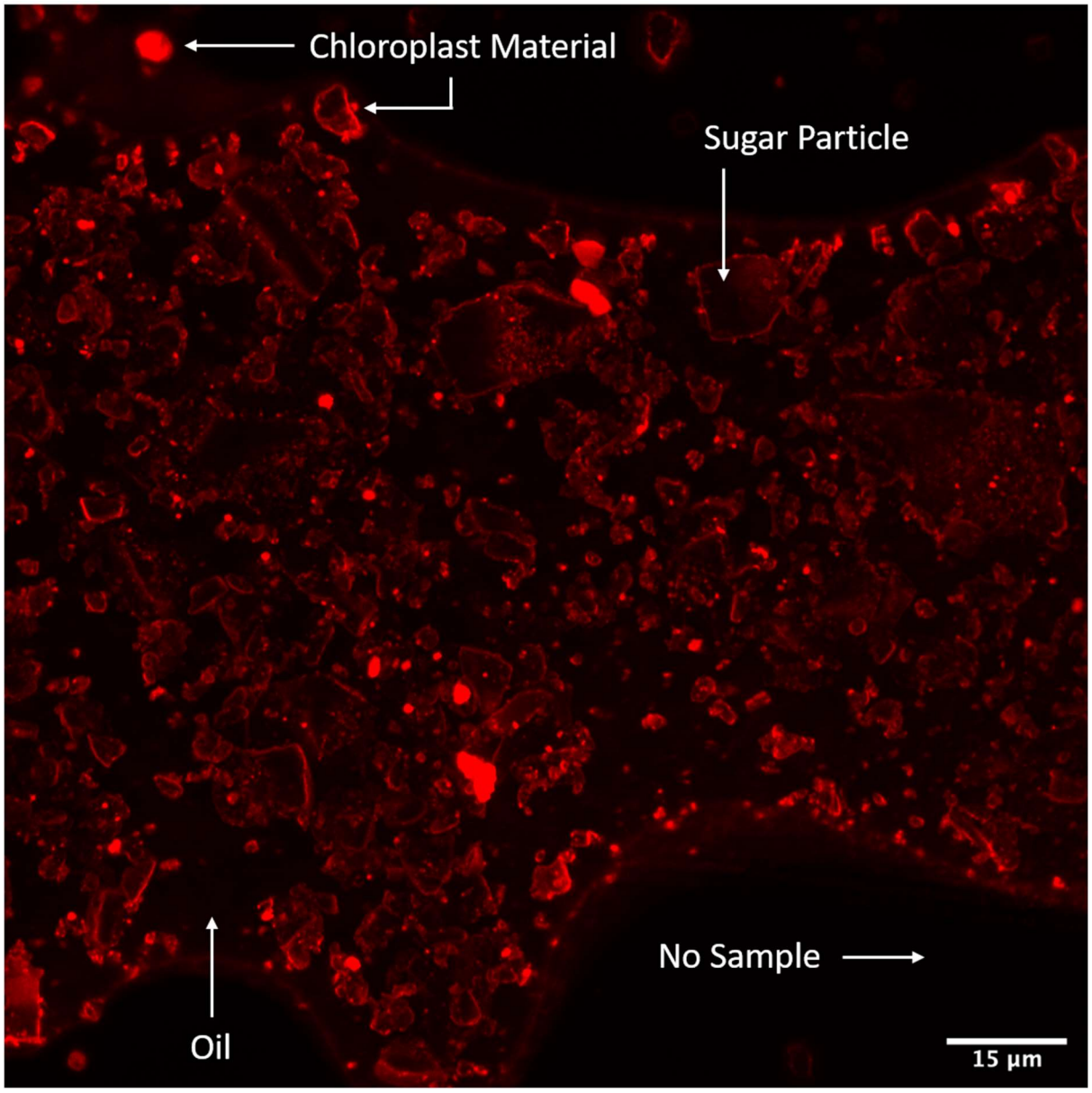

773

774 **Figure 9:** Maximum intensity projection confocal Micrographs of 1.0% S-CRF (Rhodamine B-stained
775 pellet chloroplast-rich fraction) in 50% s/o suspension at X63 objective lens (Z stacks = 20). Under 561
776 nm lamp, structures appear in red indicate the protein-stained chloroplast material (Rhodamine B,
777 λ_{ext}: 553 nm, λ_{emi}: 627 nm). Black region is area with no sample, while the lighter red region indicates
778 the oil phase. Scale bar represents 15 µm.

779

780

781